NUCLEAR MAGNETIC RESONANCE EVIDENCE USING D_2O FOR STRUCTURED WATER IN MUSCLE AND BRAIN

FREEMAN W. COPE

From the Aerospace Medical Research Laboratory, U. S. Naval Air Development Center, Warminster, Pennsylvania 18974

ABSTRACT The electric quadrupole moment of the deuterium nucleus provides a nuclear magnetic resonance (NMR) probe of electric field gradients, and thereby of organization of tissue water. 8–17% of H_2O in rat muscle and brain was replaced by D_2O from 50% deuterated drinking water. The peak height of the steady-state NMR spectrum of D in muscle water was 74% lower than that of an equal concentration of D_2O in liquid water. Longitudinal NMR relaxation times (T_1) of D in water of muscle and brain averaged 0.092 and 0.131 sec, respectively, compared with 0.47 sec in D_2O in liquid water. Transverse NMR relaxation times (T_2) averaged 0.009 and 0.022 sec in D_2O of muscle and brain, respectively, compared with 0.45 sec in D_2O in liquid water. These differences cannot be explained by paramagnetic ions or by magnetic inhomogeneities, which leaves increased organization of tissue water as the only tenable hypothesis. Evidence was also obtained that 27% of muscle water and 13% of brain water exist as a separate fraction with T_2 of D_2O less than 2×10^{-3} sec, which implies an even higher degree of structure. Each of the two fractions may consist of multiple subfractions of differing structure.

INTRODUCTION

The classical picture of the cell as a membranous bag containing a solution of small ions and proteins in aqueous solution is widely accepted. A contrary view of a minority regards the cell as an organized, nonliquid phase, consisting of macromolecules embedded in a matrix of semicrystalline water. The evidence for, and implications of, the minority view have been reviewed by Ling (1, 2), Troshin (3, 4) and Cope (5, 6, 7).

Clear evidence of the structure of cell water should help to resolve this controversy. Unfortunately, the long history of study of cell water structure has yielded ambiguous results, which have been interpreted in terms of liquid structure, icelike structure, or other semicrystalline structures. The earlier work has been summarized by Blüh (8), Gortner (9, 10), Weisman (11), Höber (12), and Szent-Györgyi (13).

Some pertinent literature of more recent vintage included (*a*) the suggestion by Ling (1) that intracellular water exists in the form of multiple polarized layers adsorbed upon cellular proteins, which is favored by the finding that water is adsorbed by proteins in accord with the Bradley isotherm (1, 14) and by the observation that experimentally measured cell swelling curves may be derived from this hypothesis (15), (*b*) evidence that small ions are less soluble in water of cells or actomyosin gels than in liquid water (4, 5), and (*c*) the finding that diffusion of tritium hydroxide is slower in cell water than in liquid water (16).

Nuclear magnetic resonance (NMR) seems likely to be a powerful tool for the study of the structure of cell water because NMR spectra and relaxation times are influenced by the chemical and physical environment surrounding the individual proton. Broadenings of proton NMR spectra of water have been observed in various biological materials. Approximately 75% of H of H_2O in erythrocytes has an NMR spectrum that is broadened fourfold (17). The NMR spectrum of H_2O in fish muscle shows moderate broadening (18). The NMR spectrum of H_2O in nerve shows a partial splitting into two peaks (19), or slight broadening (20). NMR relaxation times of H in muscle water were shown to be much shorter than in liquid water and to be influenced by contraction of the muscle (21). Unfortunately, the interpretation of these data is confused by the fact that broadenings of proton NMR spectra may be produced by mechanisms other than change of structure (i.e., by paramagnetic ions or by microscopic magnetic inhomogeneities caused by extended π-electron systems in biological macromolecules). Additional complications of interpretation result from the possibility that tissue water may consist of two or more fractions with different structures. Nevertheless, the above NMR studies strongly suggest that at least some of cell water has a great degree of crystallinity than liquid water.

The present study is an attempt to clarify the above interpretative difficulties, by using both steady-state and spin-echo NMR, and by substituting study of the deuterium nucleus for that of hydrogen. Because of its electric quadrupole moment, the deuterium nucleus serves as an NMR probe of microscopic *electric* fields in tissue water. In contrast, NMR study of hydrogen yields information on microscopic *magnetic* fields because hydrogen lacks a quadrupole moment. Quadrupole effects have previously extended the usefulness of NMR in studies of solids (22), and have been of value for the study of mesomorphic phases of surface active compounds (23) and of water organization by collagen (24).

In the present study, the steady-state NMR spectrum of deuterium was shown to be much lower in muscle water than in liquid water. Pulsed NMR studies of deuterium showed marked differences in NMR relaxation times between tissue and liquid water, and ruled out the possibility that these effects could be due to paramagnetic ions or to magnetic inhomogeneities. That tissue water has a significantly greater degree of crystallinity than liquid water remained the only tenable hypothesis. The existence of a second fraction of tissue water with an even shorter relaxation time and even more structure was also demonstrated. It seems probable that each of

these two fractions of tissue water may consist of multiple subfractions with different degrees of crystallinity.

METHODS

Steady-State NMR Experiments

NMR spectra of D in D_2O were obtained in a conventional manner on a Varian wide line NMR spectrometer (Varian Associates, Palo Alto, Calif.) with a setting of approximately 6140 gauss modulated sinusiodally at 20 cycles per sec with an amplitude of approximately 8.2×10^{-3} gauss peak-peak. Resonance was obtained with a radio frequency of 4×10^6 Hz adjusted to produce a rotating field (H_1) estimated at approximately 6×10^{-3} gauss in amplitude. This is the lowest value of H_1 with which it was convenient to use this instrument. Nevertheless, studies of NMR spectrum peak heights vs. H_1 showed evidence of a small amount of saturation. RC filtering of 3 sec time constant was used to reduce noise. The spectrum was scanned by slowly varying H_0 during approximately 100 sec. An average of two or more repetitions of NMR spectrum was often used in order to reduce errors due to instrumental noise. The $\pm 5\%$ tolerance resistors used by Varian on the signal level fine control (which controls the gain of the output amplifier of the spectrometer) were replaced by $\pm 1\%$ tolerance resistors which reduced analytical errors due to discrepancies between gains at different gain settings from 5 to 1%. A 3 ml volume of solution or muscle was placed in a 9 mm diameter cellulose plastic test tube which was positioned in the NMR spectrometer probe by a plastic spacer. Sample temperatures averaged 25°C during analysis.

Pulsed NMR Experiments

A 2 ml volume of solution or tissue in a glass test tube of 14 mm internal diameter was centered in the NMR probe. The experiments were performed at the NMR resonance of deuterium at 4×10^6 Hz and approximately 6140 gauss, which was produced by a 12 inch diameter Varian electromagnet.[1] A continuous 4×10^6 Hz signal was generated by a crystal oscillator which was turned on and off by a solid-state gate. The resulting radio frequency pulses were amplified by a transmitter of approximately the design of Clark (25, 26). Clark's circuit was modified to include a tuned coil in the plate circuit of the final transmitter stage, which was transformer-coupled to a 50 ohm line with a 50 ohm termination. This was connected in parallel with an NMR probe (2–4 megacycles), which was taken from a Varian wide-line NMR spectrometer. This probe has separate transmitter and receiver coils. Peak-to-peak height of the transmitted pulses measured approximately 150 v, with rise and decay times of approximately 3×10^{-6} sec. The receiver coil of the probe was coupled to a preamplifier and receiver with a voltage gain of 200 which followed approximately the design of Clark (25, 26). The receiver output was subjected to phase detection approximately in the manner of Clark (25, 26), followed by DC amplification (gain = 40 x) with an RC filter of 0.5×10^{-3} sec response time. The detector output was displayed on an oscilloscope, and 20 or 30 repetitions of the signal were averaged by a small computer in order to improve signal-to-noise ratio. The averaged signal was then plotted on paper by an X-Y recorder.

With each sample, measurements were made using 90°–90° or 90°–180° pulse pairs. The correct width of the 90° pulse was selected by adjustment to maximize the height of the free induction decay curve. The correct width of the 180° pulse was selected by adjustment to

[1] Magnet gap was 1.75 inches.

maximize the height of the echo. The 90° pulse was generally found to have a width of approximately 1×10^{-6} sec. Phase of the reference signal was matched to that of the free induction decay by adjustment for maximum height of free induction decay.

A 90°–180° pulse combination was used with various time delays in a series of experiments to record echoes at various times after the 90° pulse. From a graph of the logarithm of echo height vs. time after the 90° pulse, the time required for echo height to decay to 1/e of an earlier value was measured, thus determining transverse relaxation time (T_2). The pair of pulses was repeated once each 4 sec with liquid D_2O systems, and once each 1.3 sec with tissue samples.

Longitudinal relaxation time (T_1) was measured with a 90°–90° pulse pattern as described by Hahn (27) and Boehme and Eisner (28). Height of each free induction decay was measured at 8×10^{-3} sec after the end of the transmitted pulse. The heights of the free induction decays of the first 90° pulse alone and second 90° pulse alone were averaged. The height of the decay after the second pulse in a 90°–90° pair was then measured for various values of pulse separation (τ) and these values were each subtracted from the above average. A plot of the logarithm of each of these differences vs. τ yielded a straight line from which the time for decay to 1/e of a previous value was estimated, which provided a value of T_1. This method requires the hypothesis that the shape of the free induction decay after the second 90° pulse is independent of time between pulses (τ) which was found to be true. Free induction decays conformed approximately to a cumulative Gaussian curve.

Chemical and Biological

8–17% of muscle or brain water of adult, white, male rats was replaced with D_2O by giving the rats 50% D_2O in their drinking water for 4–5 days. At the end of this time, the rats appeared grossly normal except for moderate hypersensitivity to external stimuli. Pieces of approximately 0.5 g each of thigh muscle from a deuterated rat, killed by cervical dislocation, were packed tightly into a test tube for NMR analysis. Each brain experiment used a single rat brain with a volume of approximately 2 ml. Steady-state NMR analyses were performed within 30 min after death, and the pulsed NMR measurements were made within 1 hr after death. Concentrations of D_2O in muscle or brain water of the deuterated rats were determined by distillation of water from the tissue, followed by analysis of the distillate for D_2O by steady-state NMR. Total water concentration of muscle or brain was determined by the loss of weight after distillation at 100°C followed by lyophylization and by drying in a vacuum oven at 100°C to constant weight. Calculations of per cent visible D_2O in muscle examined by steady-state NMR used the assumption that all deuterium was in the water. The assumption of equilibrium exchange of D in D_2O with H of muscle proteins changes the results given here by only 2%. The process of distillation was shown not to change the composition of a 10% D_2O–90% H_2O mixture.

RESULTS AND DISCUSSION

Steady-State NMR Studies of D_2O in Simple Systems and in Muscle Water

The NMR resonance of pure liquid D_2O at 23° was found to be a single narrow line (Fig. 1). When D_2O was mixed with H_2O in varying proportions, a plot of peak height of the NMR spectrum of D against D_2O concentration yielded a standard curve consisting of a straight line (Fig. 2). Hence, the NMR spectrum of D may be used for quantitative analysis for D_2O in H_2O-D_2O mixtures. The NMR spectrum of

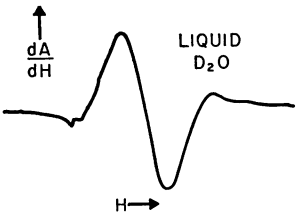

FIGURE 1 NMR spectrum of liquid D_2O. 3 ml of 99.7% pure liquid D_2O at a temperature of approximately 20°C was used. The NMR spectrum was recorded as a plot of dA/dH (the derivative of radio frequency absorption with respect to magnetic field) vs. H (magnetic field strength). The peak-peak width of this spectrum was estimated at approximately $60 \pm 30 \times 10^{-8}$ gauss.

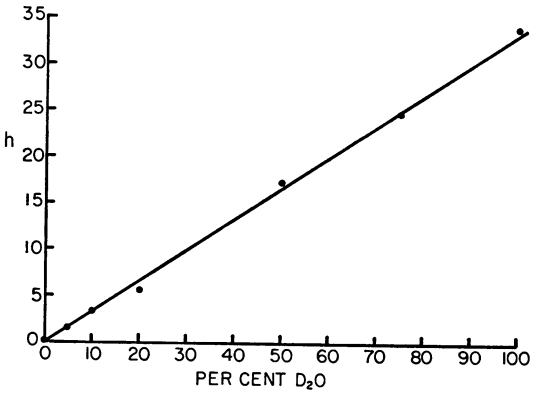

FIGURE 2 Standard curve for analysis of D_2O in H_2O. Mixtures of D_2O in H_2O were made up as per cent by volume and were analyzed for D by NMR at 20°C. On the abscissa is plotted per cent D_2O. On the ordinate, h represents the peak-to-peak height of the NMR spectrum measured for the sample, divided by the voltage gain of the output amplifier of the NMR spectrometer. Each point represents the mean of two NMR spectra on the same sample.

H has previously been used for the quantitative analysis of H_2O-D_2O mixtures (29). To learn whether small ions of biological occurrence would influence the NMR analysis of D_2O, NMR spectra were recorded for D_2O solutions on the following: 0.1 N HCl, 1 N NaOH, 1 N KCl, 0.1 N $MgSO_4$, 0.1 N K_2HPO_4, and 0.1 N citric acid. The peak heights of the NMR spectra of all of these solutions were practically unchanged from the peak height of the NMR spectrum of pure D_2O.

It seemed probable that NMR sensitivity to crystallinity might be greater with D_2O than with H_2O since the deuterium nucleus has a quadrupole electric moment which the hydrogen nucleus does not. Nuclear magnetic relaxation of H in H_2O is dominated by *magnetic* dipole interactions (30). However, nuclear magnetic relaxation of nuclei having quadrupole moments is usually dominated by the interaction of the quadrupole moment with adjacent *electric* field gradients (31, 32) and is markedly influenced by any change in these gradients, such as are to be expected with a change in crystal structure. In a liquid, electric field gradients are small because the electric dipoles of water are randomly oriented in space and randomly moving in time so that the electric fields will tend to average to zero. However, in the presence of order or crystallinity, averaging will decrease, and hence electric field gradients will increase. Therefore, crystallinity will shorten the NMR relaxation times of the deuteron and thus may broaden the line of its steady-state NMR resonance.

In agreement with the above theoretical picture, the present author observed that

TABLE I

EFFECTS OF GELATIN AND AGAR ON NMR SPECTRA OF D_2O AND H_2O

Concentration of gelatin or agar	Decrease in NMR peak height of D_2O	
%	%	
	Gelatin	*Agar*
3	—	55
5	7	67
10	9	88

Concentration of gelatin or agar	Line width of NMR spectrum of H_2O	
%	*Hz*	
	Gelatin	*Agar*
0	1.6	1.6
1	—	5.0
3	—	16.5
5	1.6	—
10	—	50.0

Data in the upper table were obtained in the present study. The peak heights of the NMR spectra of D in D_2O in the gelatin and agar gels at approximately 20°C were compared with that of pure D_2O. All preparations of gelatin and agar were observed to be in the gel state at the time of the NMR measurement. Data in the lower table were taken from the paper of Hechter et al. (42).

freezing of D_2O into ice caused disappearance of the NMR spectrum of liquid D_2O (Fig. 1), presumably due to extreme broadening. Other investigators had observed a similar disappearance (33, 34) although at sufficiently low temperature and after sufficient purification, or with single crystals, a very broad, low doublet spectrum was detected (34, 35). Its line width was approximately 1000 times that seen with liquid D_2O. On the other hand, solidification of D_2O by formation of a gel by 5 or 10% gelatin had little effect on the NMR spectrum of D (Table I). In an agar gel,

however, the peak heights of the NMR spectra of D_2O were much reduced. The relative magnitudes of the agar and gelatin effects on the D_2O spectrum paralleled the presence or absence of broadening of the NMR spectrum of H_2O in these two gels (Table I). Hence, it seems likely that both H_2O and D_2O data are manifestations of a single difference in effect between gelatin and agar on the structure of interstitial water.

A steady-state NMR study of muscle water was done. In fresh muscle of three rats in which 10, 12, and 14%, respectively, of muscle water had been replaced by D_2O, the NMR peak heights were depressed to 28, 27, and 24%, respectively, of the values to be expected from the muscle content of D_2O. This large effect might be due to crystallinity of some or all of muscle water, but perhaps also due to magnetic inhomogeneities or dissolved paramagnetic ions. To distinguish between these possibilities, it was necessary to use pulsed NMR techniques.

Pulsed NMR Experiments

General Principles. In steady-state NMR spectroscopy, the sample is irradiated continuously with radio frequency energy. In pulsed NMR techniques, however, the sample is irradiated with pulses of radio frequency energy, and radio emission is measured following the incident pulses. The instrumentation is described in the Methods section. The complicated physical theory has been well described in an elementary manner by Hahn (27) and Pople et al. (30). For a rigorous discussion, see Hahn's original paper (36).

Three different types of pulsed NMR experiments will be discussed.

First, free induction decays may be observed. When a sample of liquid D_2O is irradiated with 150 v (peak-peak) pulse of 4×10^6 Hz radio frequency energy for approximately 1×10^{-3} sec in the presence of the steady magnetic field for NMR resonance, then a millivolt radio frequency signal is emitted by the sample which starts at the end of the pulse, and which declines with a half-life of approximately 22×10^{-3} sec (Fig. 3). This general phenomenon may be predicted from the Bloch equations (36), and was first observed experimentally by Hahn (36). The shape of the free induction decay is often not describable by a simple exponential and its theoretical analysis may be quite complicated (36, 38). In a liquid, such as D_2O, free induction decay is caused primarily by inhomogeneity of the magnetic field over the sample (36). However, if transverse relaxation time (T_2) is made sufficiently short, free induction decay is determined primarily by T_2 and may be a simple exponential.

Second, one may measure the decay of the signal emitted by the sample after elimination of the effect of macroscopic magnetic inhomogeneities. The result may be called transverse relaxation time (T_2). Let us suppose that different values of magnetic field (H_0) are found in different parts of the sample, due to imperfections in the electromagnet producing H_0, or to magnetic particles in the sample. Deuterons in areas of different H_0 will then precess at slightly different frequencies and thus get

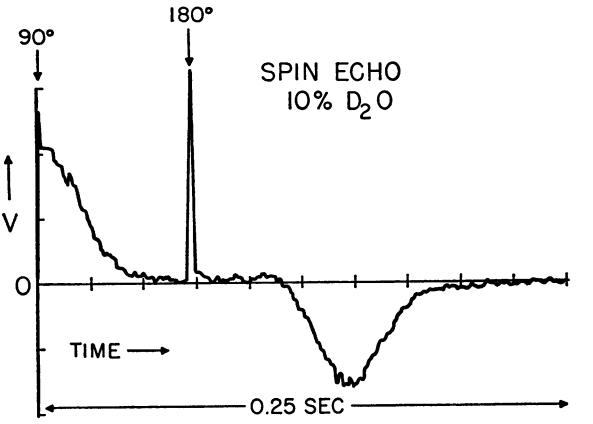

FIGURE 3 Free induction decay and echo of deuterium in 10% D_2O–90% H_2O at 24°C. Sample volume is 8 ml. Voltage (V) output of the phase detector is plotted against time. The sample is subjected to the 90° pulse (1×10^{-3} sec duration) at zero time, which is followed by emission by the sample of a free induction decay, after which the sample is subjected to a 180° pulse (2×10^{-3} sec). The echo is emitted by the sample at an equal time later.

out of phase with each other, thus causing a decay of the radio signal emitted by the sample. However, provided the change in H_0 relative to position is fairly gradual, so that the individual deuteron experiences little change in H_0 over its diffusion path during its relaxation time, the phase error accumulated by the individual deuteron is proportional to time after the first pulse. Hence, if the direction of precession of the deuteron is reversed by a 180° pulse, a phase error of opposite sign is accumulated, so that after an equal length of time, all deuterons which have been dephased by the above mechanism come back into phase for a brief time, thus emitting a pulse which is called an echo (Fig. 3). The decay of echoes therefore measures loss of coherence of precessing deuterons by mechanisms other than macroscopic magnetic inhomogeneities. Macroscopic here means larger than the diffusion path of a deuteron during one relaxation time.

Third, one may discriminate the loss of emitted radio signal due to random errors in *phase* of precession from loss due to change in *direction* of axis of precession of deuterons. By observing the height of the free induction decay after the second 90° pulse of a 90°–90° pulse pair as a function of time between pulses, one may observe the time course of return of deuterons to equilibrium axis position (called longitudinal relaxation time or T_1). T_1 is to be distinguished from T_2 in that T_2 decay is the sum of both dephasing and longitudinal flipping.

To summarize, T_1 measures decay by longitudinal flipping only, T_2 measures the sum of decay due to the sum of flipping plus any dephasing which is random causing loss of phase memory, and free induction decay is the sum of these two plus addi-

tional dephasing for which phase memory exists, due to macroscopic magnetic inhomogeneities.

Spin-Echo Behavior of Liquid D_2O Systems. Spin echoes are easily observed in liquid D_2O systems (Fig. 3). Echo decay in liquid D_2O followed a simple exponential curve (Fig. 4) from which T_2 was determined. Decay of the height of the free induction decay after the second pulse of a 90°–90° pattern also conformed to a single exponential (Fig. 5) in accord with the theory of Hahn (36), and from which T_1 was measured. Free induction decay shape conformed approximately to a cumulative Gaussian curve with respect to time.

In deoxygenated 100% D_2O at 25°C, T_1 had an average value of 0.41 sec (Table II), which agrees satisfactorily with the value of 0.45 sec obtained by interpolation from the data of Woessner (39). T_1 measurements were then made on liquid D_2O systems under conditions more nearly like those in tissues. The results in Table II show that dissolved air, dilution of D_2O in H_2O, or the addition of 1 N NaCl had only small effects on T_1 of D in D_2O.

T_2 of 10% D_2O–90% H_2O in air was observed to be 0.45 sec, which is similar to

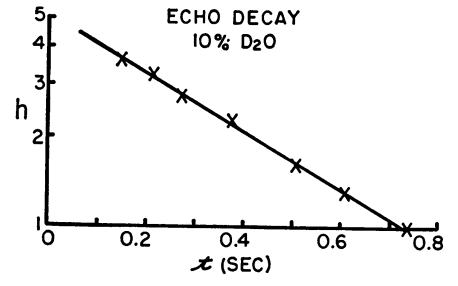

FIGURE 4 Echo decay for 10% D_2O. Sample was 2 ml of 10% D_2O–90% H_2O in air at 24.5 C. Height (h) of the echo following the 90°–180° pulse pattern was measured as a function of time (t) between the echo and the 90° pulse. h is expressed in arbitrary units. h on a log scale is plotted against t. From the line drawn through the data points, T_2 is estimated to be 0.45 sec, which is the time for h to decay to 1/e of a previous value.

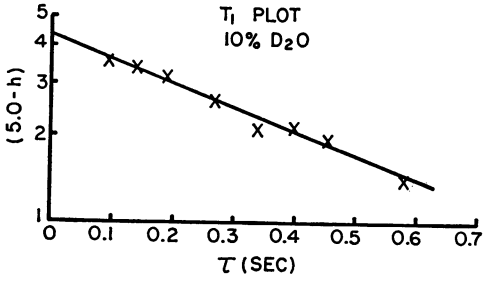

FIGURE 5 T_1 plot for 10% D_2O. Sample was 2 ml of 10% D_2O–90% H_2O in air at 24°C. Height (h) of the free induction decay of the *second* pulse of a 90°–90° pulse pattern was measured as a function of time (τ) between pulses (h is measured in arbitrary units). Height of free induction decay of *first* pulse was measured equal to 5.0. (5.0–h) on a log scale is plotted against τ. From the line drawn through the data points, T_1 is estimated to be 0.53 sec, which is the time for (5.0–h) to decay to 1/e of a previous value.

TABLE II

T_1 AND T_2 FOR LIQUID D_2O SYSTEMS

Sample	T_1 (sec)		T_2 (sec)	
	data	mean	data	mean
100% D_2O (O_2 free)	Woessner (39)	0.45		
100% D_2O (O_2 free)	0.44, 0.37, 0.43, 0.35, 0.42, 0.43	0.41		
100% D_2O (in air)	0.41, 0.40, 0.42, 0.41, 0.48	0.42		
10% D_2O – 90% H_2O (in air)	0.42, 0.42, 0.48, 0.49	0.47	0.45, 0.45, 0.45, 0.45, 0.44	0.45
1 N NaCl in 10% D_2O – 90% H_2O	0.53, 0.49, 0.51	0.51	0.40, 0.44, 0.39	0.41

Temperature = 25° ± 1°C. The data of Woessner (39) shows that for 100% D_2O (O_2 free), log (T_1) is linearly related to the reciprocal of absolute temperature over a moderate range. The value given in the first line was obtained from the data of Woessner (39) by interpolation on that basis.

TABLE III

T_1 AND T_2 FOR D_2O IN MUSCLE AND BRAIN

Type of tissue	Rat No.	D_2O in tissue water	Temp.	T_1	T_2
		%	°C	*sec*	*sec*
Muscle	1	8	28	0.123	0.009
"	2	10	28	0.120	0.008
"	3	14	25	0.080	0.009
"	4	12	26	0.105	0.009
"	5	14	22	0.050	0.009
"	6	14	23	0.075	0.009
"	Mean	12	25	0.092	0.009
Brain	7	14	25	0.140	0.027
"	8		23	0.140	0.009
"	9		25	0.135	0.036
"	10		26	0.110	0.015
"	Mean	14	25	0.131	0.022

With rats No. 7 and 9, T_2 was determined from decay of echoes after 90°–180° pulse pattern. With other rats, T_2 was so short that the free induction decay interfered with their measurement. In these cases, T_2 was measured from $t_{1/e}$ of the free induction decay. Per cent D_2O in tissue water was determined on the muscle samples individually, but together on the four pooled brains.

the value of T_1 (Table II). Addition of 1 N NaCl produced only a small reduction (Table II). No data on T_2 of D_2O could be found in the literature for comparison.

Spin-Echo Behavior of D_2O in Muscle and Brain. T_1 plots for D_2O in muscle and brain were well described by single exponential decays. T_1 for D_2O in muscle and brain averaged 0.092 and 0.131 sec, respectively (Table III), which contrasts with the value of 0.47 sec in 10% D_2O in liquid water (Table II).

T_2 of D_2O in muscle and brain was even shorter than T_1, and was even more different from that observed in liquid D_2O. The echo decay times were as short as, or almost as short as, the free induction decays. In Experiments 7 and 9 (Table III), echo decays were enough slower than free induction decays, so that the echoes were clearly distinguishable and echo decay curves were plotted which showed simple exponential decays from which T_2 was measured. With the other samples of muscle and brain, echo decay was as fast as, or faster than, free induction decay, so that T_2 was estimated from free induction decay times. From these estimates (Table III), T_2 for D_2O in muscle had an average value of 0.009 sec and in brain was 0.022 sec, compared to 0.45 sec in 10% D_2O in liquid water (Table II).

Interpretation of NMR Behavior of D_2O in Tissues

Our problem is to decide whether the NMR behavior of D_2O in tissues is due to paramagnetic ions, or to magnetic inhomogeneities, or to a structure of tissue water different from that of liquid water.

Since paramagnetic ions affect the steady-state NMR spectrum and T_1, and are present in tissues, they might be responsible for the NMR characteristics of D in tissue water. This possibility was evaluated by a brief experimental study of the effects of paramagnetic ions on the NMR behavior of D_2O. First, the effects of various concentrations of various paramagnetic ions on the peak height of the steady-state NMR spectrum of D in D_2O were observed (Table IV). Paramagnetic ions lowered peak heights (Table IV), but had little effect on line widths. Second, T_1 and T_2 were studied as a function of Mn^{++} concentration in D_2O (Fig. 6). The simple theory of Bloembergen et al. (40) for H_2O predicts that T_1 is inversely proportional to paramagnetic ion concentration, and hence predicts a straight line with a slope of one in a log-log plot of T_1 vs. Mn^{++} concentration. The experimental results for T_1 in D_2O (Fig. 6) show approximately a straight line but the slope is *not* equal to one. This difference is probably due to the fact that a quadrupolar mechanism contributes to the T_1 relaxation of D_2O but not of H_2O for which the theory was designed. T_2 also shows linearity for D_2O (Fig. 6). In the presence of Mn^{++}, T_2 for D_2O is considerably shorter than T_1, which was also observed for H_2O containing Mn^{++} by Zimmerman (41).

Qualitative considerations do not allow a decision regarding the possibility that NMR effects in tissue D_2O might be due to paramagnetic ions, since in both cases peak height of the steady-state spectrum is lowered and T_1 and T_2 are shortened.

TABLE IV

EFFECT OF PARAMAGNETIC IONS ON PEAK HEIGHT OF NMR SPECTRUM OF D_2O

Concentration of paramagnetic ion	Salt used for NMR experiment	μ_{eff} (Bohr magnetons)	Reductions in peak ht. of NMR spectrum of D_2O
			%
0.1 M Cu^{++}	$CuSO_4$	2.0	5
0.1 M Cr^{+++}	$CrK(SO_4)_2$	3.8	67
0.1 M Fe^{+++}	$FeCl_3$	5.9	50
0.1 M Mn^{++}	$MnCl_2$	5.9	82
0.01 Cr^{+++}	$CrK(SO_4)_2$		15
0.001 Cr^{+++}	$CrK(SO_4)_2$		4
0.01 Fe^{+++}	$FeCl_3$		0
0.001 Fe^{+++}	$FeCl_3$		0
0.01 Mn^{++}	$MnCl_2$		24
0.001 Mn^{++}	$MnCl_2$		10

Peak heights of spectra of D in 100% D_2O solutions of various paramagnetic ions were compared with that of pure D_2O at 20°C. Magnetic moments (μ_{eff}) for different paramagnetic ions as determined by susceptibility measurements are taken from data summarized on p. 209 of Pople et al. (30).

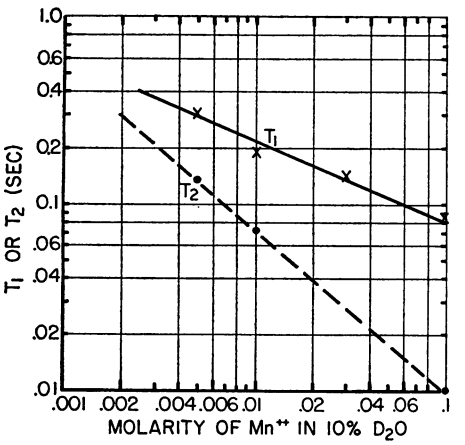

FIGURE 6 T_1 and T_2 vs. $[Mn^{++}]$ in D_2O. Various concentrations of $MnCl_2$ are dissolved in 10% D_2O–90% H_2O. $T = 25° \pm 1°C$.

However, *quantitative* considerations reveal that paramagnetic ions cannot be responsible for the NMR behavior of D_2O in tissues. From Fig. 6, it is evident that approximately 0.07 M Mn^{++} would have to be present in tissues to shorten T_1 to 0.1 sec, which is approximately the value observed in tissues. Other paramagnetic ions or free radicals of physiological occurrence have equal or smaller magnetic moments than Mn^{++}, and hence would require equal or higher concentrations to produce this effect on T_1. Concentrations in muscle of Fe, Cu, and Mn are reported to be 3×10^{-4}, 2×10^{-5}, and 2.5×10^{-6} M of wet muscle, respectively (43, 44, 45), and free

radical concentration is approximately 5×10^{-5} M (46). Therefore, total concentration of paramagnetic ions in muscle is approximately 3.7×10^{-4} M, which is approximately 200 times too small to cause the short value of T_1 observed in D_2O in muscle.

Magnetic inhomogeneities due to extended π-electron systems in DNA molecules have been said to be the cause of broadening of the NMR spectrum of H of H_2O in DNA gels (47). To study this effect in D_2O, a minute quantity of finely powdered iron metal was introduced into a sample of liquid D_2O. This produced a maximum of magnetic inhomogeneities accompanied by a minimum of particle surface effects, because the gigantic ferromagnetism of iron metal allowed substantial magnetic inhomogeneities to be produced by vanishingly small quantities of iron. The minute quantity of iron powder decreased the peak height of the NMR spectrum of D in D_2O by 70%. Therefore, it was clear that microscopic magnetic inhomogeneities in muscle and brain, if present, would indeed lower the NMR spectrum of D_2O in tissue water. However, the short values of T_1 of D_2O observed in water of muscle or brain can *not* be due to magnetic inhomogeneities, because the theory of spin echo NMR indicates with certainty that magnetic inhomogeneities cannot alter T_1 (36). The NMR behavior of D_2O in tissue water must therefore be caused by conditions other than magnetic inhomogeneities.

Since the paramagnetic ion and magnetic inhomogeneity hypotheses have been eliminated, the only hypothesis which remains tenable is that electric field gradients are much larger in cell water than in liquid water, which must reflect a difference in structure of muscle water compared to liquid water. Because NMR relaxation of quadrupolar nuclei occurs predominantly by interaction of the quadrupole electric moment of the nucleus with surrounding electric field gradients (31, 32) we can neglect the magnetic dipole mechanisms responsible for relaxation of H in H_2O. In a liquid, electric gradients will be small because the electric dipoles of water are randomly oriented in space and randomly moving in time so that the electric field at any time and in any position will tend to average to zero. However, order or crystallinity will reduce such averaging and hence will increase electric field gradients, and thus provide a mechanism for rapid NMR relaxation of deuterons, such as is observed in water of muscle and brain. Hence, order or crystallinity must be significantly greater in water of muscle and brain than in liquid water.

We may ask whether the water in muscle or brain is homogeneous in structure or consists of two or more fractions with different structures.

As a first approach to this question, we shall seek to learn whether the free induction and T_2 decay curve observed in muscle represents *all* of muscle water or only a fraction thereof. The T_2 decay curve of muscle D_2O showed a single exponential decay down to approximately 2×10^{-3} sec after the 90° pulse (Fig. 7). For shorter times, the decay curve could not be mapped accurately because of instrumental limitations. Therefore, the possibility remained of a second fraction of muscle water

with T_2 less than 2×10^{-3} sec. The possible existence of such a fast fraction was tested indirectly by determining whether the free induction decay of muscle D_2O was large enough to account for all of the D_2O proven to be present in the muscle.

The height of the beginning of the free induction decay in liquid D_2O-H_2O without additives was easily determined by direct measurement because of the gaussian shape and relatively slow decay. This height vs. D_2O concentration in D_2O-H_2O mixtures gave a linear standard curve (Fig. 8), which shows that the height of the free induc-

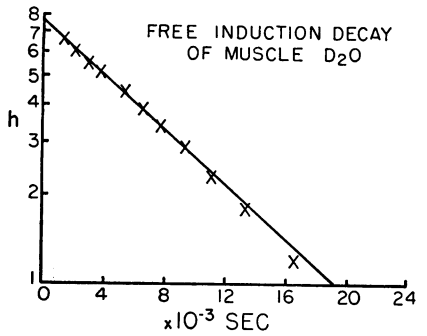

FIGURE 7 Free induction decay of muscle D_2O. Time in milliseconds after a single 90° pulse is plotted on the abscissa. *h* represents voltage emitted by the sample in arbitrary units, which is plotted on a logarithmic scale on the ordinate. Sample is 2 ml of rat muscle at 24°C measured within 1 hr post-mortem. The muscle water contains 14% D_2O by volume. Decay for the muscle sample is much faster than for liquid D_2O (compare Fig. 3), which is caused by a short value of T_2. Therefore, muscle free induction decay reflects primarily T_2 decay, and becomes almost simple exponential, instead of gaussian as seen with liquid D_2O.

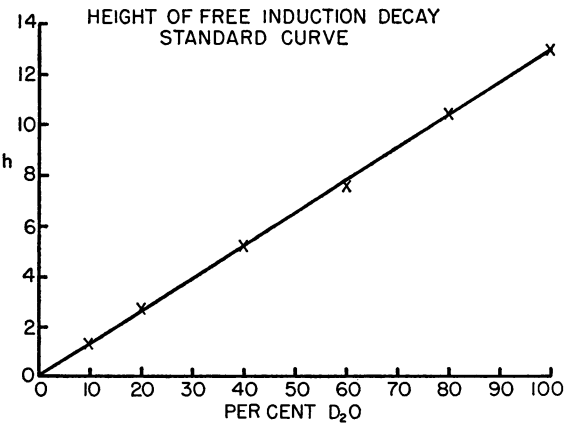

FIGURE 8 Standard curve of free induction decay height vs. D_2O concentration. Mixtures of D_2O in H_2O were made up as per cent by volume and were studied at 23°C. On the abscissa is plotted per cent D_2O. On the ordinate, *h* represents the height of the beginning of the free induction decay, after a 90° pulse. *h* has been corrected for differences in receiver gain used on the different measurements. Each free induction decay curve is an average of 20 repetitions of the same experiment.

tion decay is suitable for quantitative analysis for D_2O in D_2O-H_2O mixtures. To see whether the analysis remained accurate when free induction decay was short, 0.1 N Mn^{++} was added, which made free induction approximately as short as in muscle. Under these conditions, free induction decay became simple exponential in shape, so that a linear semilog plot of the free induction decay of D_2O could be extrapolated to zero time to obtain the initial height. Initial heights of the free induction decays in 15% D_2O—85% H_2O without and with 0.1 N Mn^{++} were respectively 4.8, 4.8, 4.7, 4.8, 4.9, (mean = 4.8), and 4.8, 4.9, 5.1, 4.7, 4.8, 5.2, (mean = 4.9) in the same arbitrary units. This indicates that the quantitative estimation of D_2O concentration from height of the free induction decay remains accurate when decay is as short as in muscle.

These procedures were applied to fresh muscle samples from six different deuterated rats. Muscle D_2O free induction heights were compared with those of a 10% D_2O–90% H_2O standard. D_2O concentration in the muscle was calculated from steady-state NMR analysis for D_2O concentration in distilled muscle water, together with measurement of the dry weight of each muscle sample. Muscle water was replaced by 14, 17, 18, 19, 18, and 19% D_2O, respectively, in the six muscle samples. The heights of free induction decays observed in the six muscle samples were smaller than those to be expected from the concentrations of D_2O contained in the samples. The observed deficits of 10, 29, 36, 32, 30, and 26%, respectively, (mean = 27%) must measure the size of a second fraction of muscle water with T_2 shorter than 2×10^{-3} sec. Similar experiments with rat brain yielded estimates of 11, 13, 32, and −3% (mean = 13%) for the size of a fraction of water with very short T_2. Brain water was replaced by 17, 16, 22, and 12% by D_2O, respectively, in the four brain samples.

One may therefore infer the existence of two distinct fractions of tissue water with markedly different values of T_2, both of which are much shorter than T_2 of liquid water. Exchange of water molecules between the two fractions must be relatively slow; otherwise, the decay of the slow fraction would fail to be the observed simple exponential (Fig. 7). The limitation on exchange between the two fractions suggest that the fractionation results from compartmentation at the anatomic level, rather than from layering at the molecular level. In the latter case, exchange between fractions would be expected to be fast because of the small distances between fractions relative to the diffusion path of a water molecule. The anatomic locations of the two fractions of water cannot be judged from the data of this paper.

It is possible that each of the two fractions of tissue water is not homogeneous, but may consist of two or many subfractions with different structures. The observation that in the slower fraction of water of muscle and brain, T_2 is much shorter than T_1 suggests either (*a*) a distribution of correlation times (48), which implies a distribution of water structures, or (*b*) a rapid exchange of protons between two or more subfractions with different chemical shifts (30, pp. 218–222), or both. Possibly there may be two subfractions consisting of an icelike subfraction of protein hydra-

tion shells comprising less than 1% of total water plus a large liquid fraction, as postulated by Bratton et al. (21) to explain their spin-echo data on H in muscle water, which resemble the data for the slower component of T_2 of D_2O in muscle. The experiments of Bratton et al. (21) were not designed to reveal the possible existence of a second fast component of T_2 Bratton et al. (21) admitted that their data could also be explained by the hypothesis of a continuous distribution of water structures, but failed to consider this possibility further. The present author believes that the continuous distribution of structures is the more likely hypothesis, because it has been found to explain well spin-echo NMR data of water in other protein systems (49, 50), and because it is suggested by adsorption isotherms of water on proteins (2, 14), and by cell hydration data (15).

Received for publication 3 October 1968.

Note Added in Proof. Using steady-state NMR analysis of H_2O, Hazlewood et al. have reached conclusions that resemble closely those of the present study. They provide evidence for at least two fractions of muscle water with different degrees of structure, but both with significantly more structure than liquid water. The minor fraction (approximately 8% of total water) is believed to have an extremely high degree of structure. (Hazlewood, C. F., B. L. Nichols, and N. F. Chamberlain. *Nature*. Submitted for publication.)

REFERENCES

1. LING, G. N. 1962. A Physical Theory of the Living State. Blaisdell Publishing Co., Waltham, Mass.
2. LING, G. N. 1965. *Ann. N. Y. Acad. Sci.* **125**:401.
3. TROSHIN, A. S. Problems of Cell Permeability. Original Russian edition published in Moscow. 1956. German translation published by Gustav Fischer Verlag, Jena. 1958. Revised English edition published by Pergamon Press, Ltd., London, England. 1966.
4. TROSHIN, A. S. 1961. *In* Membrane Transport and Metabolism. A. Kleinzeller and A. Kotyk, editors. Academic Press Inc. Ltd., London, England.
5. COPE, F. W. 1967. *J. Gen. Physiol.* **50**:1353.
6. COPE, F. W. 1967. *Bull. Math. Biophys.* **29**:691.
7. COPE, F. W. 1970. *Advan. Biol. Med. Phys.* **13**: in press.
8. BLÜH, O. 1928. *Protoplasma.* **3**:81.
9. GORTNER, R. A. 1930. *Trans. Faraday Soc.* **26**:678.
10. GORTNER, R. A. 1932. *Annual Rev. Biochem.* **1**:21.
11. WEISMANN, O. 1938. *Protoplasma.* **31**:27.
12. HÖBER, R. 1945. Physical Chemistry of Cells and Tissues. Blakiston Co., Philadelphia, Pa.
13. SZENT-GYÖRGYI, A. 1957. Bioenergetics. Academic Press, Inc., New York.
14. HOOVER, S. R., and E. F. MELLON. 1950. *J. Amer. Chem. Soc.* **72**:2562.
15. COPE, F. W. 1967. *Bull. Math. Biophys.* **29**:583.
16. LING, G. N., M. M. OCHSENFELD, and G. KARREMAN. 1967. *J. Gen. Physiol.* **50**:1807.
17. ODEBLAD, E., B. N. BHAR, and G. LINDSTRÖM. 1956. *Arch. Biochem. Biophys.* **63**:221.
18. SUSSMAN, M. V., and L. CHIN. 1966. *Science.* **151**:324.
19. CHAPMAN, G., and K. A. MCLAUCHLAN. 1967. *Nature.* **215**:391.
20. FRITZ, O. G., and T. J. SWIFT. 1967. *Biophys. J.* **7**:675.
21. BRATTON, C. B., A. L. HOPKINS, and J. W. WEINBERG. 1965. *Science.* **147**:738.
22. COHEN, M. H., and F. REIF. 1957. *In* Solid State Physics, Volume 5. F. Seitz and D. Turnbull, editors. Academic Press, Inc., New York.

23. FLAUTT, T. J., and K. D. LAWSON. 1967. In Magnetic Resonance and Relaxation. R. Blinc, editor. North-Holland Publishing Co., Amsterdam, The Netherlands.
24. MIGCHELSEN, C., and H. J. C. BERENDSEN. 1967. In Magnetic Resonance and Relaxation. R. Blinc, editor. North-Holland Publishing Co., Amsterdam, The Netherlands.
25. CLARK, W. G. 1961. Pulsed Nuclear Magnetic Resonance in Alkali Halides. Ph.D. Thesis, Physics Department, Cornell University, Ithaca, New York.
26. CLARK, W. G. 1964. *Rev. Sci. Instr.* **35**:316.
27. HAHN, E. L. 1953. *Phys. Today.* **6**:4.
28. BOEHME, H., and M. EISNER. 1967. *J. Chem. Phys.* **46**:4242.
29. MITCHELL, A. M. J., and C. PHILLIPS. 1956. *Brit. J. Appl. Phys.* **7**:67.
30. POPLE, J. A., W. G. SCHNEIDER, and H. J. BERNSTEIN. 1959. High-Resolution Nuclear Magnetic Resonance. McGraw-Hill Book Company, New York.
31. SHIMIZU, H. 1964. *J. Chem. Phys.* **40**:754.
32. BONERA, G., and A. RIGAMONTI. 1965. *J. Chem. Phys.* **42**:175.
33. JACKSON, J. A., and S. W. RABIDEAU. 1964. *Bull. Amer. Phys. Soc.* **9**:142.
34. JACKSON, J. A., and S. W. RABIDEAU. 1964. *J. Chem. Phys.* **41**:4008.
35. WALDSTEIN, P., S. W. RABIDEAU, and J. A. JACKSON. 1964. *J. Chem. Phys.* **41**:3407.
36. HAHN, E. L. 1950. *Phys. Rev.* **80**:580.
37. HAHN, E. L. 1950. *Phys. Rev.* **77**:297.
38. BLOOM, A. L. 1955. *Phys. Rev.* **98**:1105.
39. WOESSNER, D. E. 1964. *J. Chem. Phys.* **40**:2341.
40. BLOEMBERGEN, N., E. M. PURCELL, and R. V. POUND. 1948. *Phys. Rev.* **73**:679.
41. ZIMMERMAN, J. R. 1954. *J. Chem. Phys.* **22**:950.
42. HECHTER, O., T. WITTSTRUCK, N. MCNIVEN, and G. LESTER. 1960. *Proc. Nat. Acad. Sci. U.S.A.* **46**:783.
43. SCOTT, E. M., and R. H. MCCOY. 1944. *Arch. Biochem. Biophys.* **5**:349.
44. EGGLETON, W. G. E. 1940. *Biochem. J.* **34**:991.
45. REIMAN, C. K., and A. S. MINOT. 1920. *J. Biol. Chem.* **42**:329.
46. COMMONER, B., J. TOWNSEND, and G. E. PAKE. 1954. *Nature.* **174**:689.
47. BALAZS, E. A., A. A. BOTHNER-BY, and J. GERGELY. 1959. *J. Mol. Biol.* **1**:147.
48. ODAJIMA, A. 1959. *Progr. Theoret. Phys. Suppl. 10.* 142.
49. CLIFFORD, J., and B. SHEARD. 1966. *Biopolymers.* **4**:1057.
50. KRÜGER, G. J., and G. A. HELKE. 1967. In Magnetic Resonance and Relaxation. R. Blinc, editor. North-Holland Publishing Co., Amsterdam. The Netherlands.